INVESTIGATION ON THE PETROPHYSICAL CHANGES ON A COQUINA CORE UNDER CARBONATE WATER INJECTION ASSISTED BY COMPUTERIZED TOMOGRAPHY

[1]Eric Yuji Yasuda, [2]Erika Tomie Koroishi, [3]Osvair Vidal Trevisan and [4]Janeth Alina Vidal Vargas
[1]Master's Student – Mechanical Engineering, State University of Campinas, UNICAMP
[2,4]Researcher – Center for Petroleum Studies – CEPETRO
[3]Professor – Department of Energy, State University of Campinas – UNICAMP.

This paper was prepared for presentation at the International Symposium of the Society of Core Analysts held in Vienna, Austria, 27 August – 1 September 2017.

ABSTRACT

Multiple interactions between injected fluid and the reservoir rock occur during oil recovery processes. These interactions are particularly important if CO_2 is used as injection fluid either in enhanced oil recovery (EOR) methods or in CO_2 sequestration projects in deep saline aquifers, especially in carbonate reservoirs. When CO_2 dissolves in water, carbonic acid (H_2CO_3) is formed. The resulting acid water will react with the carbonate salts, calcium carbonate ($CaCO_3$) and magnesium carbonate ($MgCO_3$) present in the reservoir rock, causing its dissolution. This effect is expected to change the main properties of the reservoir, such as permeability and porosity. This work proposes an experimental investigation on the permeability and porosity changes of a pressurized carbonate rock with the injection of brine saturated with CO_2. Tomography is used to observe the behavior of any wormholes created during the test. The experiment was carried out at 2,000 psi, 18^{o}C and four different flow rates of 0.025, 0.075, 0.1 and 2 cc/min. Results show that the porosity had a constant increase during the experiment, with a steeper increase on the end of the experiment when the flow rate was higher. Overall permeability showed an increase of about twenty times the initial value. Local permeability showed a similar behavior for each of the sections of the rock, with a reduction at lower flow rates and an increase at higher ones. Some regions had final permeability of up to 4D, an indicator of a wormhole. Tomography highlighted the creation of a wormhole in the beginning of the core.

INTRODUCTION

The acidization and the process of wormhole propagation have been studied by many researchers. Grigg and Svec [1] showed that the injection of CO_2 in carbonate rocks increases the permeability of the sample close to the injection point, due to the formation of a wormhole, and that in the fluid production region the permeability was reduced due to the damage caused by the precipitation of calcium carbonate. These inferences highlight the importance to control these effects in order to prevent problems, such as clogging the fluid production or bypassing the oil region near the injection point. The findings of this work are related to the rate of the injection fluid, which is higher at the injection point and slower at the production region because of the energy loss while the fluid flows through the reservoir.

The effect of injection rate on the patterns of dissolution was studied through the injection of water into plaster made cores. Also, it was found out an optimal value to form a wormhole as prominent feature. At a high injection rate, the acid has less time to dissolve the rock so that the permeability of the core will not be increased. At low injection rates, the acid has more time to dissolve the rock and therefore to create larger voids near the wellbore, which may cause borehole collapse during production [2,3]. These conditions are not optimal, and cost more acid to create a wormhole. This was corroborated by Hoefner and Fogler [4] with experiments using limestone and dolomite cores. The optimal injection rate decreased as the acid-rock reaction changed from mass transfer control to reaction kinetics control, as described in the results from the experiments of Fredd and Fogler [5]. Other parameters as medium heterogeneity, acid concentration and core size were also studied [6, 7, 8, 9].

Golfier et al. [10] found through experiments that the shape of the wormholes is based on two dimensionless numbers; Péclet (Pe) and Damköhler (Da), the first relates the advection to the diffusion and the second relates the chemical reaction rate to the transport phenomena. These numbers are among other factors, based on the flow rate of injection and the properties of the porous medium. They also created a classification for the different types of wormholes based on its form.

This work proposes an experimental investigation on the permeability and porosity variations of a coquina core subjected to a carbonate water injection. The experimental parameters are: 2,000 psi of both radial and axial pressures, 18°C, flow rates of 0.025; 0.075; 0.1 and 2 cc/min. A special coreholder with multiple pressure taps along the length of the core is used in order to evaluate the permeability, the porosity is evaluated through computerized tomography and validated by monitoring the calcium concentration of the production fluids.

PROCEDURES

Materials

The carbonate rock used in the study was extracted from a coquina outcrop in the CIMPOR (former Atol) quarry, from Morro do Chaves formation, in the Sergipe-Alagoas basin, Brazil. Three fluids were employed in the experiment: an equilibrated brine at 38 kppm salt concentration as the initial saturation fluid, a sodium iodide (NaI) brine at 38 kppm as the dopant and an equilibrated brine at 38 kppm saturated with CO_2 at 2,000 psi as injection fluid. Table 1 shows the equilibrated brine composition, and it was designed to have no chemical interaction with the core sample.

Table 1. Equilibrated brine composition.

	NaCl	KCl	$MgCl_2 \cdot 6H_2O$	$CaCl_2 \cdot 2H_2O$	$SrCl_2 \cdot 6H_2O$	KBr	Na_2SO_4	$NaHCO_3$
Mass of each component [g/L]	31.288	0.781	0.276	5.403	0.018	0.107	0.176	0.059

Methods

The experimental setup is the same used in the earlier project of 2015 [11], a positive displacement pump, high pressure vessels, a special coreholder with multiple pressure taps, a backpressure system and differential pressure transducers. The coreholder is designed for X-ray tomography, with an aluminum cylinder, with an epoxy and carbon fiber jacket around the sample. The experimental apparatus is schematized in Figure 2.

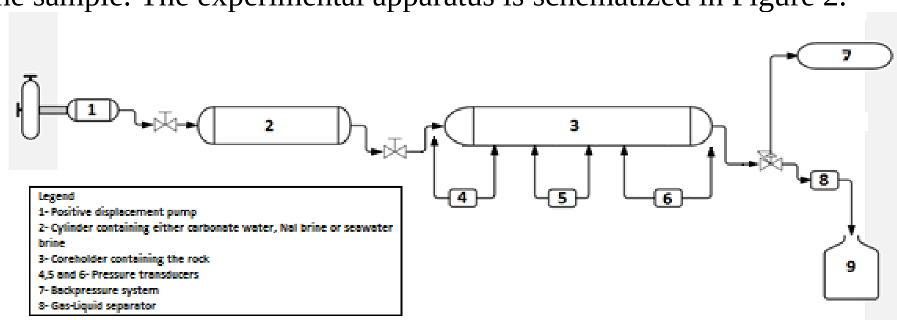

Figure 2. Scheme of the experimental apparatus.

After each carbonate water injection cycle, the sample was flushed with the equilibrated brine in order to isolate the effect of each flow rate. The equilibrated water was injected at 2 cc/min after each flow rate swap until the sample was totally saturated and ready for the next experimental step. Differential pressures were measured at points along the core as shown in the Figure 2 by the transducers (nVision Crystal Engineering Corporation). These ensured the permeability evaluation through the sample length. The pressure was measured in six points and enabled five permeability sections of the rock, presented in Figure 3 by K0, K1, K2, K3 and K4.

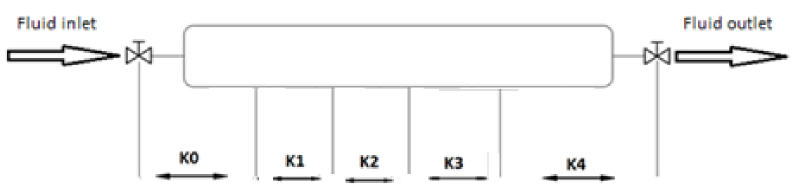

Figure 3. Scheme of the permeabilities evaluated during the test.

Porosity was evaluated by X-ray computerized tomography (Siemens CT scanner model SWFVD30C), using the software Syngo. The images had a 0.5 mm resolution and each scan acquired 69 images along the sample. It was also evaluated, in order to confirm the results, by the analysis of calcium concentration of the production fluid.

RESULTS

Porosity

Tomography Method

A MatLab™ routine, developed by Vargas, was used in order to verify the porosity changes. The mean porosity obtained through the CT values is shown in Figure 4. The absolute variation was from 12.27% to 13.69%. The variation was steady, with a slightly greater increase at the beginning, until the high flow rate of 2 cc/min when the porosity increased substantially.

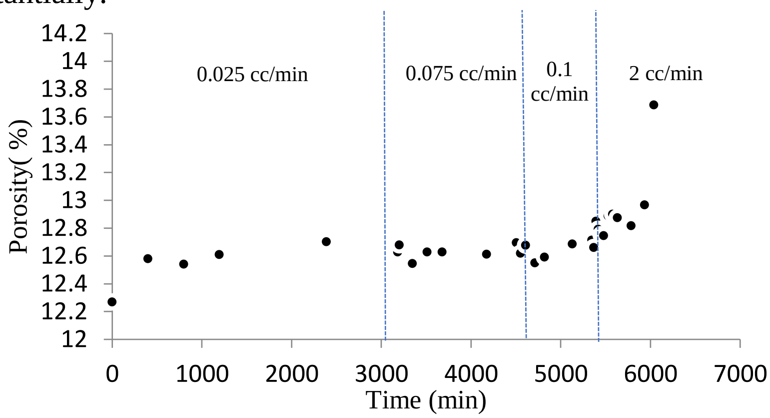

Figure 4. Porosity through time by tomography method.

Calcium Concentration Method

The porosity values obtained from the CT scans were validated by the calcium concentration method. This method evaluates the amount of calcium dissolved on the production fluid by inductively coupled plasma-optical emission spectrometry (ICP-OES), the analysis was carried out by the analytic central from the Chemistry Institute of UNICAMP. Considering the outcrop rock is composed by calcite, the calcium variation can be converted in pore volume variation using Equations 2 and 3 from Mangane [12]:

$$\phi(t) = \phi_0 + \frac{100.V_{CaCO3}(t)}{V} \quad (2)$$

$$V_{CaCO_3}(t) = \frac{(\Delta Ca.Q.\Delta t.M_{CaCO_3})}{M_{Ca}.\rho_{CaCO_3}} \quad (3)$$

$V_{CaCO3}(t)$ is the volume of calcite dissolved, ΔCa is the variation of the calcium concentration on the production fluid, Q is the flow rate, Δt is the time interval, M_{CaCO3} is the molar mass of the calcium carbonate, M_{Ca} is the molar mass of calcium, ρ_{CaCO3} is water density, $\phi(t)$ is porosity along time, ϕ_0 is initial porosity. The results obtained are shown in Figure 5, where the porosity changed from 12.27% to 13.69%.

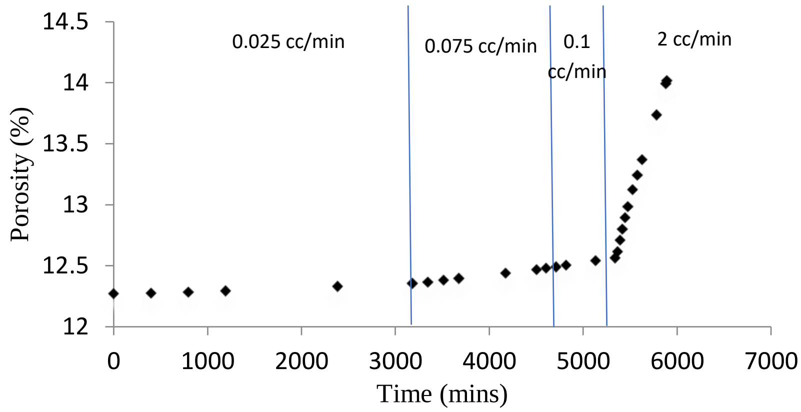

Figure 5. Porosity through time by calcium concentration method.

The methods used to calculate porosity variation presented a similar value. The first method (CT method) showed a variation of 1.75% on porosity, and the second (calcium concentration method) provided 1.42%. The flow rate of 2 cc/min had less experimental time, but injected more acid, hence the steeper increase in the porosity. Also, the higher flow rate probably damaged the porous medium, increasing the pore volume.

Permeability

The permeability had a similar behavior for all the sections, the profile showed a decrease at the beginning of the experiments, when lower injection rates were used. This decrease can be explained by precipitation of minerals. By the end of the experiment the permeability increased, because the dissolution is predominant. The sections near the injection point (K0, K1, K2) showed a much higher increase in permeability, because of the creation of a wormhole. Figure 6 shows the permeability variation for the five sections of the rock, divided by flow rates, where A=0.025 cc/min, B=0.075 cc/min, C=0,1 cc/min, D=2 cc/min.

The observed effect can be related in a field scale, to regions near the injection well for 2 cc/min high flow rate and to regions far from the injection well for the slower flow rates of 0.025 cc/min, 0.075 cc/min and 0.1 cc/min.

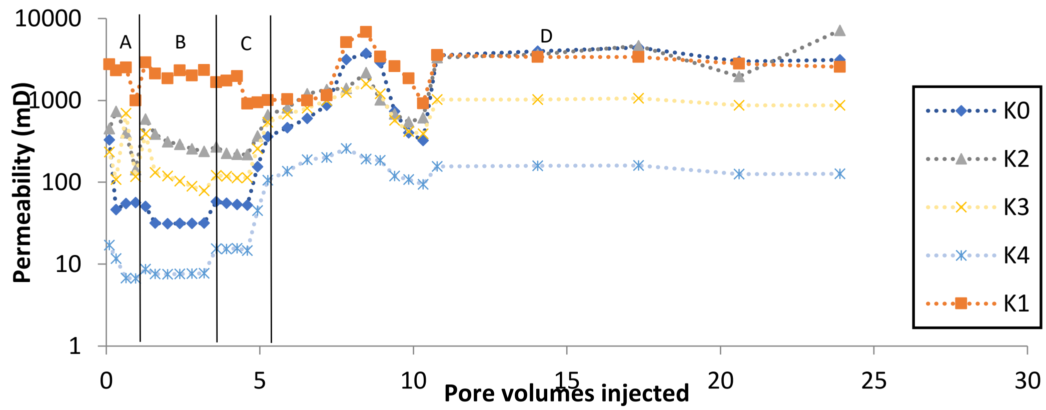

Figure 6. Mean permeability by pore volumes of carbonate water injected.

Damköhler and Péclet numbers

Both Da and Pe numbers were evaluated for this experimental work. Gharbi [13] proposed a method to estimate accurately the Da number using well-established data in the literature. Plummer et al. [14] determined the dissolution rate of calcite in well-controlled batch reactions for different CO_2 saturations and temperatures, but not considering high pressures or brines as in this experiment. Assuming that the reaction rate is related mostly on pH and temperature, it is possible to use Plummer et al.'s data to estimate the reaction rate and by consequence the Da number. This work's conditions were 18^{o}C and the pH was approximately 4.6, using Figure 8 from Plummer et al. [14] the reaction rate is $1*10^{-5}$ moles m^2s^{-1}. The pore-grain area of interface was evaluated through Brunauer–Emmett–Teller(BET) method, with a value of 0.6137. Calcite density is known, and so is its molar mass. Diffusion coefficient for the ion Ca^{2+} is $7.5*10^{-10}$ m^2/s [14]. Using the data acquired in the experiments and the approximations of Gharbi [13] it is possible to estimate the Da and Pe numbers with the following equations:

$$L = \frac{\pi.Vb}{S} \tag{4}$$

Where, L is the specific length, Vb is the bulk volume and S is the area of the pore-grain interface.

$$u_{avg} = \frac{Q}{A.\Phi} \tag{5}$$

$$Pe = \frac{u_{avg}.L}{De} \tag{6}$$

u_{avg} is the average interstitial velocity of the flow, Q is the flow rate, A is the area perpendicular to the flow, Φ is the porosity, Pe is the Péclet number, De is the diffusion coefficient for Ca^{2+},

$$k = \frac{r}{\rho.M.L} \tag{7}$$

Where, k is a reaction rate measured in units of inverse time s^{-1}, ρ is the density of calcite, M is the molar mass of calcite.
If the Pe number is higher than one:

$$Da = \frac{k.L}{u_{avg}} \tag{8}$$

If Pe number is lower than one:

$$Da = \frac{k.L^2}{De} \tag{9}$$

Finally, the results are shown in Table 2:

Table 2. Pe and Da numbers for the experiments.

Test Number	Flow Rate [cm³/min]	Pe	Da
1	0.025	2.94E-01	3.44E-02
2	0.075	8.77E-01	3.44E-02
3	0.1	1.16E+00	2.97E-02
4	2	2.29E+01	1.50E-03
5	2	2.23E+01	1.55E-03
6	2	2.06E+01	1.67E-03

According to Golfier et al. [10], with a Pe number ranging from 0.3 to 20.6 and Da from 0.034 to 0.002 should result in either a ramified wormhole or a dominant wormhole. Figure 7 shows the rock after the entire experiment, with what appears to be a dominant wormhole, highlighted in blue dots, near the injection side (left side of Fig. 7).

Figure 8 shows the rock before and after the experiments. The image is a section near the injection point, with the wormhole highlighted in a blue circle. At least three visible channels were created by the end of the experiment, possibly representing a ramified wormhole regime.

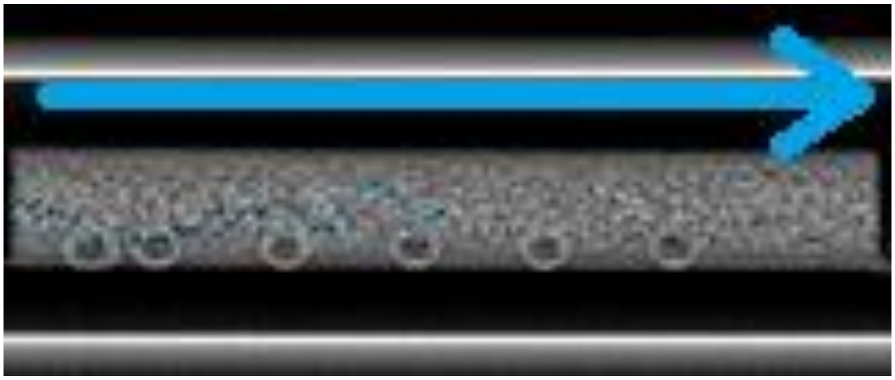

Figure 7. Tomography of the sample at the end of the experiment.

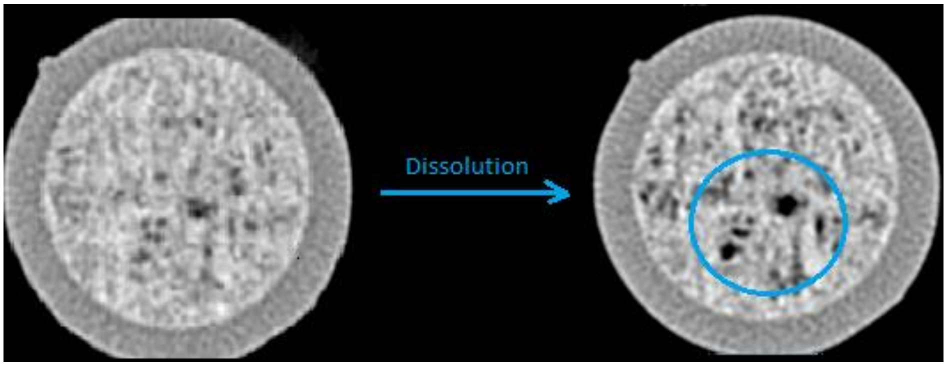

Figure 8. Cross section of the sample near injection face.

CONCLUSIONS

The results provide valuable insight to the mechanism of wormholing with injection of seawater-like brine saturated with CO_2 on carbonates. Differently from result previously shown by Yasuda et al. [11], this one provides data with very low flow rates, which simulates in the field a region far from the injection well. A porosity increase of 1.75% was evaluated by the CT scan method and 1.42% through analysis of calcium concentration of the effluents. The porosity showed a linear increase at the first 6 pore volumes injected (5,300 mins), but then there was bigger change at the injection rate of 2 cc/min. The images provided by CT scan show a wormhole at the beginning of the core, where permeability showed the greatest increase.

ACKNOWLEDGEMENTS

The authors acknowledge PETROBRAS and CNPq for financial support of the present study.

REFERENCES

1. Grigg, R.B., Svec, R.K., Lichtner, P.C., Carey, W., Lesher, C.E., CO2/Brine/Carbonate Rock Interactions: Dissolution and Precipitation, presented at the Fourth Annual Conference on Carbon Capture & Sequestration, (2005) Alexandria, Virginia, May 2-5.
2. Daccord, G., Lenormand, R., Lietard, O., Chemical dissolution of a porous medium by a reactive fluid-1. model for the “wormholing” phenomenon, *Chemical Engineering Science*, (1993) **48**, 1, 169–178.
3. Daccord, G., Lenormand, R., Lietard, O., Chemical dissolution of a porous medium by a reactive fluid-2.Convection vs reaction, behavior diagram, *Chemical Engineering Science*, (1993) **48**, 1, 179–186.
4. Hoefner, M.L., Fogler, H.S., Pore evolution and channel formation during flow and reaction in porous media, *AIChE Journal*, (1998) **34**, 1, 45-54.
5. Fredd, C.N., Fogler, H.S., Optimum conditions for wormhole formation in carbonate porous media: influence of transport and reaction, *SPE Journal*, (1999) **4**, 3, 196–205.
6. Frick, T.P., Mostofizadeh, B., Economides, M.J., Analysis of radial core experiments for hydrochloric acid interaction with limestones, presented at SPE International Symposium on Formation Damage Control, (1994) Lafayette, Louisiana, 7–10 February, SPE27402.
7. Bujise, M.A., Mechanisms of Wormholing in Carbonate Acidizing, presented in the International Symposium on Oilfield Chemistry, (1997) Houston, Texas, February 18-21.

8. Bazin, B., From matrix acidizing to acid fracturing: a laboratory evaluation of acid/rock interactions, *SPE Production and Facilities Journal*, (2001) **16**, 1, 22-29.
9. Ott, H., Pentland, C.H., Oedai, S., CO_2-brine displacement in heterogeneous carbonates, presented at the International Symposium of the Society of Core Analysts (2014), France, Avignon, September 8–11.
10. Golfier, F., Zarcone, C., Bazin, B., On the ability of a Darcy-scale model to capture wormhole formation during the dissolution of a porous medium, *Journal of Fluid Mechanics*, (2002) **457**, 1, 213-254.
11. Yasuda, E. Y., Blini, E. T. K., Trevisan, O. V., Bonet, E. J., Study of Petrophysical Properties Alterations of Carbonate Rocks under Carbonate Water Injection, presented in International Symposium of the Society of Core Analysts (2015), Canada, St. John’s Newfoundland and Labrador, August 16-21.
12. Mangane, P. O., Caractérisation des changements dans les propriétés de réservoir carbonaté induits par une modification dans la structure des pores lors d’une injection de CO2: application au stockage géologique du CO2, phD Thesis (2013), Sciences de Techniques du Languedoc-Roussillon, Universite Montpellier II.
13. Gharbi, O., Fluid-Rock Interactions in Carbonates: Applications to CO2 Storage, phD Thesis (2014), Qatar Carbonates and Carbon Storage Research Centre Department of Earth Science and Engineering, Imperial College London.
14. Plummer, L.N., Wigley, M.L., Parkhurst, D.L., The kinetics of calcite dissolution in CO2 – water systems at 5o to 600C and to 0.0 to 1.0 atm CO2, *American Journal of Science*, (1978) **278**, 1, 179-216.